7650 *Macromolecules* **2010**, *43*, 7650–7656
DOI: 10.1021/ma1013447

Macromolecules
ARTICLE

Electrospun Nanofibers with Associative Polymer−Surfactant Systems

Sachin Talwar,[†] Arjun S. Krishnan,[†] Juan P. Hinestroza,[‡] Behnam Pourdeyhimi,[§] and Saad A. Khan*,[†]

[†]*Department of Chemical and Biomolecular Engineering, North Carolina State University, Raleigh, North Carolina 27695,* [‡]*Department of Fiber Science and Apparel Design, Cornell University, Ithaca, New York 14853, and* [§]*College of Textiles, Carolina State University, Raleigh, North Carolina 27695*

Received June 17, 2010; Revised Manuscript Received August 10, 2010

ABSTRACT: Associative polymers are unique in their structure with pendant hydrophobes attached to their hydrophilic backbone, enabling associations between the hydrophobes and forming junctions in aqueous solutions. In this study, we examine efforts to produce electrospun nanofibers of associative polymers in conjunction with a readily spinnable polymer. Scanning electron micrograph (SEM) images reveal that the solution rheology sets an upper limit to the concentration of associative polymer that can be successfully electrospun. However, addition of nonionic surfactants to the precursor solution results in significant improvement in nanofiber morphology as evinced from reduced beading. Through judicious use of nonionic surfactants to modulate solution viscoelastic properties, we are able to obtain defect-free nanofiber morphology and gain new insights into the fundamentals of the electrospinning process. In particular, we find that solution viscoelasticity as measured in terms of the relaxation time, rather than viscosity as typically hypothesized, controls the nanofiber formation process.

1. Introduction

Associative polymers containing pendant hydrophobic groups are generating significant interest owing to their ability to be used in a myriad of applications ranging from paints and coatings to drug delivery. The scope and utility of these polymers can be further broadened by developing fiber-based structures for applications in nonwoven surface modification. A powerful option in this regard is to develop electrospun nanofibers of these materials, which due to their very high surface to volume ratio, would render these materials useful in many areas such as membrane technology, smart textiles, and tissue scaffolds for regenerative medicine.[1−11]

Electrospinning is a versatile technique in which a charged fluid jet from a polymer solution or melt undergoes uniaxial stretching in presence of an applied electric field and is deposited on a collector as nanofibers.[5] A large number of polymer/solvent systems have been successfully spun into fibers by employing this technique.[5,6,10] The resulting fiber diameters are usually in the submicrometer range as opposed to conventional fiber spinning techniques where the typical fiber diameters are in the order of micrometers.[12] This characteristic size scale—which imparts the fiber mats a high specific surface area and small pore size—has led to significant interest in developing novel functional electrospun materials for applications including, but not limited to, filtration devices, protective clothing and reinforced composites.[2,13,14]

However uniform fibers are not obtained from all polymer solutions. The morphology of the electrospun fibers is affected by solution properties that include viscosity, conductivity and surface tension as well as process parameters that include the precursor solution flow rate and electric field intensity. McKee et al.[15] have shown that a sufficient degree of overlap between polymer chains is necessary to obtain uniform fibers. They reported that the characteristics of the nanofibers produced via electrospinning are a strong function of the polymer concentration. While polymer droplets and beaded nanofibers are obtained from spinning at low polymer concentrations, electrospinning at higher concentrations results in the formation of bead-free nanofibers. The authors also found that, for most of the copolymers studied, C_e, the critical entanglement concentration, was the minimum concentration required for production of beaded nanofibers, while 2−2.5 times C_e was the minimum concentration required to produce uniform, defect-free fibers. The role of entanglements in electrospinning has subsequently been recognized in several other publications.[16,17] An alternate route to obtain uniform fibers at concentrations below C_e has been suggested by Rutledge and co-workers[18] wherein they introduce a high molecular weight polymer to the precursor solution in order to impart sufficient elasticity and increased relaxation time to electrospin. Interestingly, in this study, we find relaxation time to be equally significant, but one has to reduce it to obtain electrospinnability.

Associative polymers are distinctive in their structure, with hydrophobes attached to their hydrophilic backbone, enabling associations between the hydrophobes and forming junctions in aqueous solutions. We have chosen hydrophobically modified alkali-soluble emulsion (HASE) polymer, a comb-like associative polymer for this study. HASE polymers consist of a copolymer backbone with pendant hydrophobic groups, also named polymer hydrophobes (Figure 1). The polymer hydrophobes are alkyl groups attached to the backbone through a urethane linkage and separated from it by a poly(ethylene oxide) (PEO) spacer; the entire structure is referred to as a macromonomer.[19] In neutral and/or alkaline aqueous media, HASE polymers form a transient network consisting of both intra- and intermolecular hydrophobic junctions resulting in a substantial viscosity enhancement of the solution.[20−22] As such, these polymers are typically used as rheology modifiers and several studies are being undertaken to decipher the precise role of hydrophobic interactions in solution rheology. However, no effort has been made to electrospin these

*To whom correspondence should be addressed. E-mail: khan@eos.ncsu.edu. Telephone: 919-515-4519. Fax: 919-515-3465.

 Published on Web 08/18/2010 © 2010 American Chemical Society

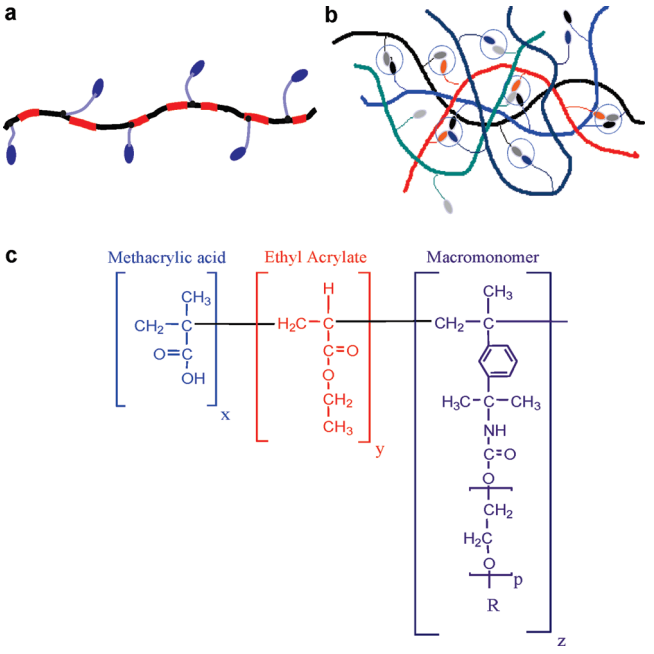

Figure 1. Schematic representation of HASE associative polymer: (a) polymer molecule by itself consisting of hydrophobes shown in blue; (b) HASE polymer in aqueous solution showing inter and intramolecular association of the hydrophobes; (c) molecular structure.

types of polymers. Electrospinning these polymers will not only open a route to the development of novel materials from associative polymers but also provide new insights into the role of rheology during the electrospinning process. Moreover, addition of surfactants to these polymer solutions can further affect their rheological properties by modulating the hydrophobic interactions in solution.[23−28] Depending on the concentration and the type of surfactant, the viscosity as well as viscoelastic properties of the HASE solutions either increase or decrease upon surfactant addition. These observations have been explained in terms of formation of mixed micelles incorporating both surfactant and polymer hydrophobes.[23,25,29]

Our goal in this study, therefore, has been to examine effective strategies for electrospinning associative polymers. This work builds on our previous study which showed that incorporation of a small amount of associative polymer facilitates electrospinning of systems typically not electrospinnable.[30] In this case though, we examine issues pertaining to the associative polymer itself: Critical questions we seek to answer include:: can associative polymers be electrospun by itself and/or in combination with other polymers, and if so, what are the concentration limits as dictated by solution rheology? Does modulation of hydrophobic interactions through surfactant addition play any role in electrospinning, and, what is the role of viscosity and viscoelasticity in the formation of nanofibers? Are surfactants present in the final fibers, and if so, how do they affect the crystallinity of the resulting fibers?

2. Materials and Methods

The HASE polymer, a copolymer of methacrylic acid, ethyl acrylate and a macromonomer with a mole ratio 43.57/56.21/0.22 respectively, was obtained from UCAR emulsion systems (Dow Chemical, Cary, NC). The macromonomer is composed of a poly(ethylene oxide) (PEO) spacer with 40 mols of EO units and a C_{22} alkyl group, and is linked to the backbone via a urethane linkage. The HASE polymer was supplied in the form of aqueous latex at a solid concentration of approximately 26% and has a molecular weight of approximately 250 kDa.[23] All impurities and unreacted chemicals were removed from the aqueous latex by dialyzing it against deionized water using a Spectrapore cellulosic membrane (cut off MW = 10000) for 3 weeks. The dialyzed latex was then liophilized for 2 days under 100 mTorr of vacuum to obtain the HASE polymer in a powder form. The pH of HASE solutions was set between 7.0 and 7.5 by adding 0.1 M NaOH. Nonylphenol ethoxylates (NPe) nonionic surfactant, Tergitol was supplied by Dow Chemical (Cary, NC) and used as received.

PEO (MW 600 kDa) was obtained from PolySciences Inc., and used as received. After preparing the polymer/surfactant samples, they were placed in a water bath overnight at 50 °C to remove entrained air and then left for 48 h at room temperature prior to rheological measurements. Rheology of the samples was measured within 3 weeks of the preparation to avoid possible polymer degradation in the presence of NaOH.[31]

All rheological experiments were performed at $T = 25$ °C in a TA Instruments AR-2000 stress controlled rheometer using a cone and plate geometry. Since the steady shear response of HASE polymer/surfactant systems is sensitive to shear history,[27] a preshear was applied at a strain rate of 5 s^{-1} for 180 s followed by a rest period of 120 s. A dynamic stress sweep test was performed to determine the limit of linear viscoelastic regime, which was thereafter utilized to perform the dynamic frequency sweep test. Low shear viscosity was determined by measuring viscosity at 10^{-1}Pa consistent with previous work on these systems.[25]

The electrospinning setup consisted of two parallel aluminum plates. A Harvard Apparatus syringe pump controlled the polymer flow to a capillary nozzle attached to one of the plates while the resulting nanofibers were collected on the other plate. A high voltage power supply (0−30 kV) was used to create a potential difference between the two plates. Our experiments were conducted with an applied field of 17−20 kV, a tip to collector distance of 20 cm, and flow rate of 15 μL/min. The electrospun fibers were gold sputtered and SEM images were obtained using a Hitachi S-3200 scanning electron microscope. The average fiber diameter was determined by measuring fiber diameters of individual fibers (at least 150) from multiple SEM images using ImageJ software. FT-IR measurements were performed on a Nicolet Magna-IR 750 FTIR spectrometer. DSC measurements on the electrospun fibers were conducted using a TA Instruments Q2000 calorimeter by heating the samples from 25 to 90 °C in a nitrogen environment at a heating rate of 10 °C/min.

3. Results and Discussion

3.1. Electrospinning of HASE with PEO. As a first step, we tried electrospinning HASE polymer by itself at concentrations above its C_e. The C_e for HASE polymers in water has been reported to occur around 0.85 wt %[32,33] at which the low shear viscosity of the solution becomes too high to allow electrospinnig. Attempts to electrospin above this concentration only resulted in the electrospraying of small droplets even at high electric fields. An effective strategy to overcome similar problems is to blend the non-electrospinnable polymer with polymers that are well suited for electrospinning.[34] On the basis of this approach, we prepared aqueous solutions of HASE polymers with poly(ethylene oxide) (PEO) of molecular weight (MW) 600 kDa. Initial electrospinning experiments were conducted on 4 wt % PEO samples containing different HASE polymer amounts. Scanning electron microscope (SEM) images of the resulting fibers reveal the positive role of HASE polymer on fiber quality (Figure 2) without any significant impact on fiber size and distribution. The mean fiber diameter for all samples studied lies between 180 and 210 nm, with a standard deviation of 30−40 nm. An improvement is noted for concentrations up to 0.1 wt % of HASE apparently due to an increase in conductivity owing to polyelectrolyte nature of HASE molecule. However an

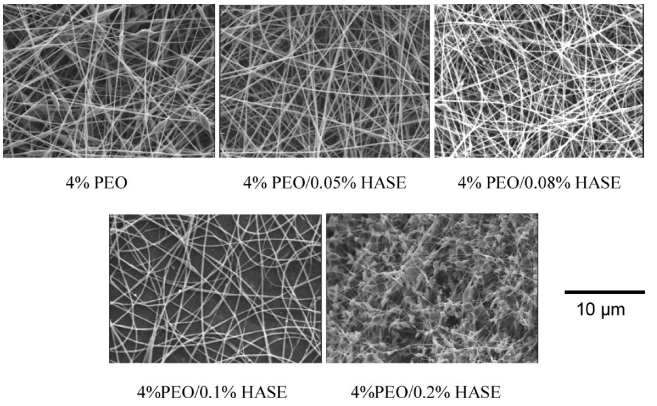

Figure 2. SEM micrographs of nanofibers from polymer solutions with 4 wt % PEO with different HASE concentrations.

increase in bead-density is obvious at concentrations higher than 0.1 wt % indicating the presence of a critical HASE concentration in order to achieve defect-free nanofibers. Moreover, there exists an upper limit (0.2 wt % in this case) of the HASE concentration above which no fibers are obtained at any values of electric fields. The occurrence of beads is mostly attributed to an increase in surface tension which in turn favors increase in surface area leading to bead-formation versus fibers. However this is not the case with our systems. The surface tension of 0.2% HASE/4% PEO solution is 62 dyn/cm which similar to that of 4% PEO (65 dyn/cm) hence ruling out surface tension as the cause for bead formation with addition of HASE.

Steady state and dynamic rheological experiments were conducted on the PEO/HASE polymer solutions to assess the role of low shear viscosity as well as viscoelastic properties on the properties of electrospun nanofibers. Figure 3a shows the low shear viscosity versus HASE polymer concentrations in 4 wt % (600 kDa) PEO solution. We find the low-shear viscosity to increase with increasing HASE concentration and exhibit three distinct regions within the range of HASE concentration studied. In the first region, the viscosity of the solution does not vary upon the addition of HASE polymer. In the second region the viscosity of the solution increases and the slope of the viscosity curve exhibits a power-law behavior. As the concentration further increases the slope changes to a higher value and that range of concentration constitutes the third region. We found that electrospinning of precursor solutions containing HASE concentrations corresponding to those in the third region resulted in either beaded fibers or no fibers, attributable to their high solution viscosity. A plausible explanation is that high viscosity values inhibit formation of Taylor cone which in turn results in fiber breakup and bead formation.

The frequency spectra of the elastic (G') and viscous (G'') moduli of the polymer solutions are shown in Figure 3b. These spectra are typical of a reversible network with transient interchain interactions and the absence of any physical gelation. A transition occurs from viscous dominated response ($G'' > G'$) at low frequencies to an elastic-dominated response ($G' > G''$) at higher frequencies for both samples containing HASE polymer. We observe that addition of HASE to the PEO solution leads to an increase in both the elastic (G') and the viscous (G'') moduli over the entire frequency range studied. The value of G' at high frequencies, which gives a measure of network connectivity or number density of elastic polymer chains in solution, increases upon addition of HASE. The values of G'' (viscous modulus) remain above those of G' over most of

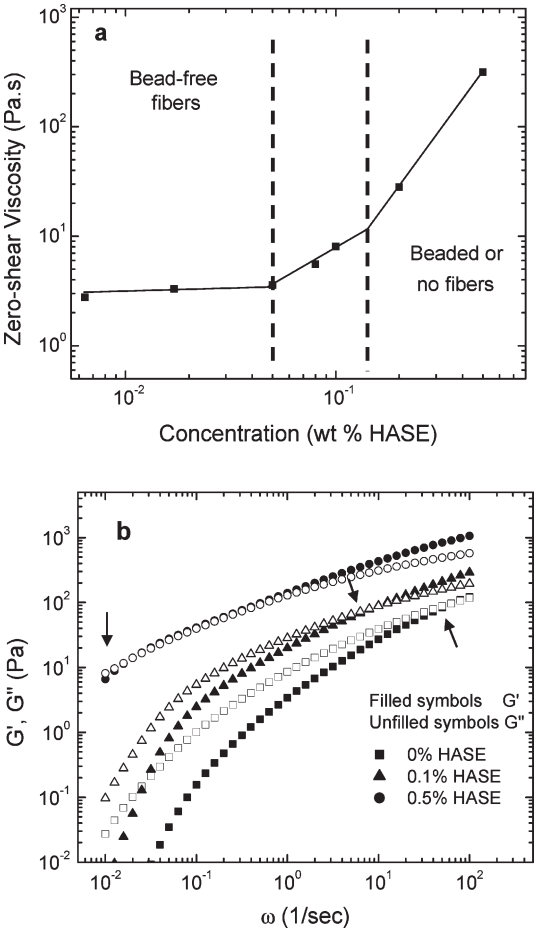

Figure 3. Steady state and dynamic rheology of polymer solutions that were electrospun. Key: (a) zero-shear viscosity versus HASE polymer concentration for 4 wt % PEO/HASE polymer solutions; (b) dynamic frequency spectrum of the elastic (G') and viscous (G'') moduli of 4% PEO/HASE polymer solutions at different HASE concentrations. The arrows correspond to crossover points.

the frequency range studied for the sample containing 0.1% HASE concentration. This concentration was the maximum concentration at which defect-free fibers could be obtained, i.e., hence indicating the dominance of the liquid-like behavior of the polymer solution. In the case of the sample containing 0.5 wt % HASE, which was not electrospinnable, the G' values were higher than those of G''. The characteristic relaxation time (τ_R) for these polymer systems can be estimated from the reciprocal of frequency (ω) at the crossover of G' over G''. We observe that the relaxation time increases by over 2 orders of magnitude as HASE concentration is increased from 0.1% to 0.5% and by about an order of magnitude when HASE concentration is increased from 0 to 0.1%. These results indicate that the viscoelastic properties, as reflected by moduli and relaxation times, along with steady state viscosity do play an important role in the electrospinning process, and they are in agreement with recent discoveries on the effect of elasticity on the formation of electrospun fibers.[35,36] However unlike other cases[18,30] where attempts are made to induce spinnability by introducing elasticity in polymer solutions at low concentrations, typically below their C_e, we find that at low HASE concentrations PEO solutions exhibit sufficient elasticity to enable fiber formation. On the other hand, we notice that high relaxation times at high HASE concentrations impede fiber formation in otherwise spinnable systems resulting either in beaded fibers or no fibers at all.

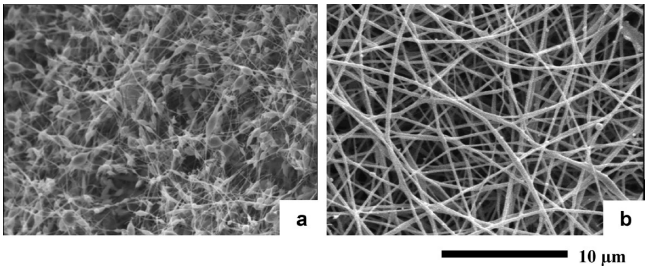

Figure 4. SEM images and solution rheology of nanofibers from PEO/HASE solutions. Fibers from solutions of 4 wt % PEO/0.2 wt % HASE both without (a) and with (b) NP15 nonionic surfactant.

3.2. Role of Surfactants. The nanofibers obtained from the solution containing 0.2 wt % of HASE polymer are of poor quality as is evident from the SEM image in Figure 2. To overcome the issue of bead formation, we resorted to the use of nonionic surfactants. The motivation behind this decision is based on previous work on associative polymers by our group[23,25] in which nonylphenol ethoxylate (NP*e*) nonionic surfactants [*e* representing the number of ethylene oxide groups in the hydrophilic headgroup], were shown to have a profound influence on the hydrophobic interactions of HASE polymers. Addition of NPe surfactants to the polymer solutions leads to a slight improvement in conductivity which can be attributed to the existence of polar groups in the NPe molecule. Parts a and b of Figure 4 show SEM images of electrospun nanofibers obtained from solutions containing 4 wt % PEO/0.2 wt % HASE with and without the presence of 20 mM NP15 nonionic surfactant. We observe a significant improvement in the fiber morphology upon addition of surfactants with a considerable reduction in bead-density. The fiber diameter was found to be 260 ± 70 nm. For the sake of clarity, we will hereon refer to the 4 wt % PEO/0.2 wt % HASE solution without surfactant as w/oNP15, and with surfactant as w/NP15. We selected NP15 as a representative surfactant because it is the most hydrophilic of the ones we examined earlier, and has the most influence in rheology;[25] effects of other surfactants are however discussed later.

Steady state and dynamic rheological experiments were conducted on both w/oNP15 and w/NP15 samples to assess the effect of the surfactant on steady shear viscosity as well as their viscoelastic properties. Figure 5a shows steady shear viscosity vs stress profile for both samples. The values of viscosity of the w/NP15 sample are lower than those of w/oNP15 except at very high stresses. Since it is unlikely that the small changes in viscosity upon surfactant addition are substantial enough to cause a drastic reduction in bead-density in the electrospun nanofibers, variations in the elastic response of this polymeric system were further examined by monitoring the evolution of G' and G'' as a function of frequency.

The frequency spectra of the elastic (G') and viscous (G'') moduli of the w/oNP15 and w/NP15 samples are shown in Figure 5b. We observe that addition of NPe leads to a decrease in both the elastic (G') and viscous (G'') moduli over the entire frequency range studied. The value of G' at high frequencies, which gives a measure of network connectivity or number density of elastic polymer chains in solution, decreases as surfactant is added to the solution. More importantly, the relaxation time τ_R decreases by almost an order of magnitude upon the addition of NP15. These results indicate that the viscoelastic properties of the polymer solution, particularly polymer relaxation time, play a crucial role in the electrospinning of this polymeric system. We speculate that NP15 surfactant serves to alter the dynamics of the polymer solution by affecting the hydrophobic interactions of

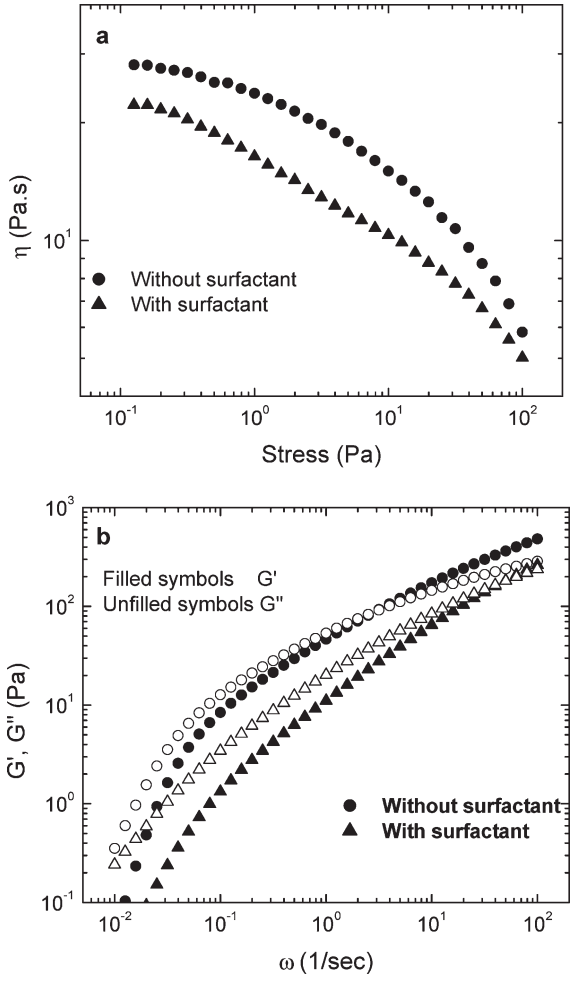

Figure 5. Steady state viscosity (a), and frequency spectrum (b) of the elastic (G') and viscous (G'') moduli for 4 wt % PEO/0.2 wt % HASE solutions with and without 20 mM NP15.

the HASE polymer in solution, resulting in lower connectivity and a lower τ_R, with the eventual outcome of reduction in bead-defects. In their work on electrospinning of Boger fluids at concentrations below C_e, Yu et al.[18] have successfully demonstrated that solution elasticity, as reflected in the relaxation time, is the critical criterion in obtaining uniform fibers. Our results serve to further complement the notion of the importance of characteristic relaxation time. Yu et al. showed that one needs to increase relaxation time for systems below C_e to achieve electrospinnability whereas in our case we find that we need to reduce relaxation time to obtain uniform fiber formation.

In order to increase the concentration of HASE in the resulting fibers, we performed electrospinning experiments on solutions with 3 wt % PEO (600 kDa) and 0.5 wt % HASE. Figures 6a and 6b show the SEM images of electrospun fibers obtained from the 3 wt % PEO/0.5 wt % HASE solutions both with and without 20 mM of NP15 surfactant. Fibers with significant amounts of beads are noted during attempts to electrospin the solution without surfactant. Upon surfactant addition, fibers with significantly improved morphology are obtained. Here again we observe a minor reduction in viscosity upon surfactant addition and a significant transformation in the trends of dynamic moduli (Figure 7). It appears that surfactant addition leads to a viscous-dominated ($G'' > G'$) behavior for the entire frequency spectrum studied as opposed to an elastic dominated regime for

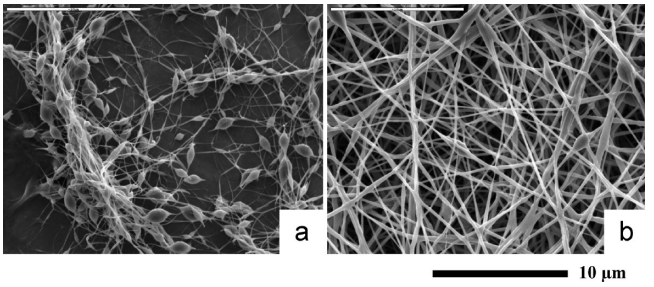

Figure 6. SEM images of nanofibers from PEO/HASE solutions. Fibers from solutions of 3 wt % PEO/0.5 wt % HASE both without (a) and with (b) NP15 nonionic surfactant.

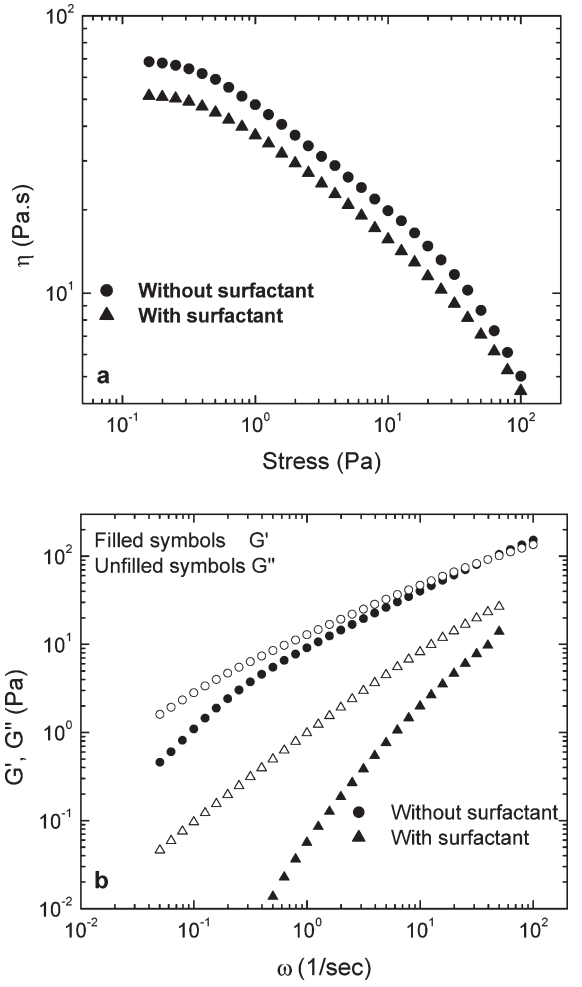

Figure 7. Steady state viscosity (a), and frequency spectrum (b) of the elastic (G') and viscous (G'') moduli for 3 wt % PEO/0.5 wt % HASE solutions with and without 20 mM NP15.

the solution without surfactants. The crossover of G' and G'' does not occur in the experimental frequency range indicating a significant decrease in τ_R upon surfactant addition. These results further corroborate the assertion that polymer viscoelasticity profoundly influences fiber morphology during electrospinning. More generally, they show that nonionic surfactants can be used to obtain electrospun nanofibers of associative polymers of this class by modulating the relaxation time of the precursor solutions. It should be noted that addition of surfactants may lead to lowering of surface tension but we ruled this out as a factor by conducting controlled experiments to isolate the effect.

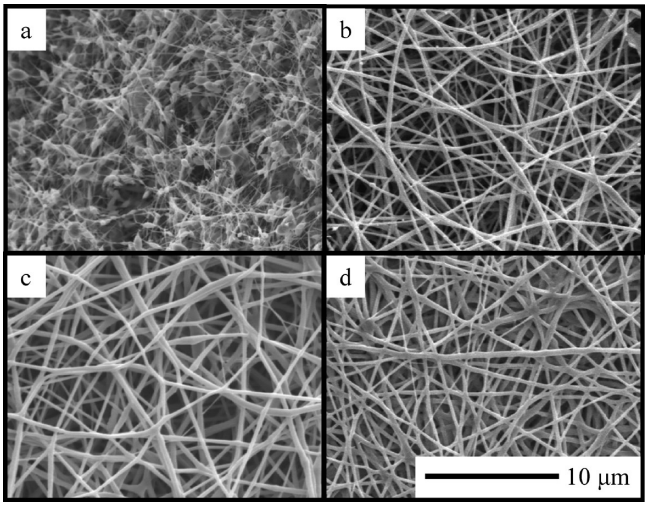

Figure 8. SEM images of nanofibers from PEO/HASE solutions. Fibers from solutions of 4 wt % PEO/0.2 wt % HASE (a) without nonionic surfactant, and with 20 mM of surfactants (b) NP15, (c) NP12, and (d) NP8.

The universality of nonionic surfactants in facilitating fiber formation is demonstrated by considering surfactants belonging to the same homologous series (NPe) but having different amphiphilicities, described by the hydrophilic–lipophilic balance (HLB) which is a measure of the weight fraction of the hydrophilic portion of a surfactant molecule. The effect on fiber quality of addition of 20 mM of NP15, NP12 and NP8, in order of decreasing HLB, to 4% PEO/0.2% HASE solutions is shown in Figure 8. In all cases, upon addition of surfactant, remarkable improvement in fiber quality is obtained. The fiber mean diameter varies between 330 to 270 nm, with a standard deviation of approximately 80 nm. These observations further substantiate our contention of the relationship between viscoelasticity and electrospinnability. Previous studies have shown that the three surfactants studied have a qualitatively similar effect on the rheology of associative polymer solutions at surfactant concentrations used here.[25]

3.3. FTIR Spectroscopy of Electrospun Nanofibers. An important consideration in electrospinning multicomponent polymer systems is to determine the presence of the polymer of interest in the resulting fibers. We sought to establish the presence of HASE polymer in the nanofibers by directly exposing the fiber mat to infrared beam in transmittance mode. The FTIR spectra of the fibers spun from pure PEO solutions are expected to exhibit characteristic peaks around 1100 and 962 cm^{-1} which are associated with the stretching of the C−O—C group present in the PEO molecule.[37] Figure 9 shows the FTIR spectra of the nanofibers obtained from pure PEO solutions as well as those spun from precursor solutions containing PEO and HASE. Also shown in Figure 9 is the spectrum of nanofibers obtained from PEO/HASE solutions containing NP15 surfactant. For the sake of clarity, the figure does not represent the entire IR spectrum but only the wavelength range where new peaks were observed upon addition of either HASE or the NP15 surfactant. The presence of HASE in the fibers from PEO/HASE solutions can be verified by the appearance of new characteristic peaks corresponding to the frequencies associated with the stretching of C═O of the ester group (1730 cm^{-1}) and COO^- group (1580 cm^{-1}) present in the chemical structure of HASE molecule.[38] In the case of fibers obtained from PEO/HASE/NP15 solutions, we notice a new peak at 1513 cm^{-1}, apparently due to the presence of para-substituted

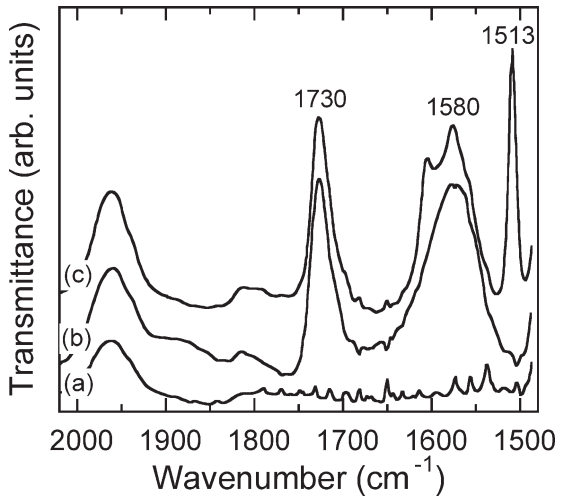

Figure 9. FT-IR spectra for fibers obtained from electrospinning solutions with different components. The spectra correspond to solution mixtures of either (a) PEO, (b) PEO/HASE, and (c) PEO/HASE/NP15 surfactant.

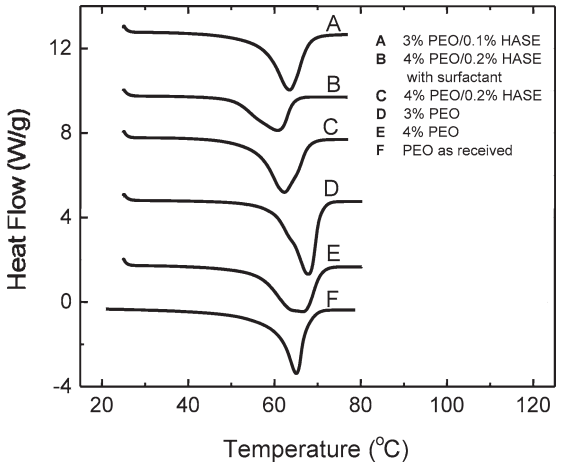

Figure 10. DSC melting endotherms of fibers spun from various samples along with "as received" PEO sample.

benzene, which is a characteristic peak in the spectrum of pure NP15 surfactant. These results confirm that the NP15 surfactants are also incorporated in the nonwoven nanofiber web along with the larger polymer molecules of PEO and HASE after the electrospinning of the solutions.

3.4. Crystallinity of Electrospun Fibers. An intriguing issue is the effect of addition of a second polymer and surfactants on the properties of the electrospun fibers in terms of their crystallinity. The percent crystallinity of the electrospun fibers was determined via differential scanning calorimetry measurements as shown in Figure 10. The area under the melting curve on the DSC plot provides the heat associated with melting for the polymer. This quantity when normalized by the polymer heat of fusion of 100% crystalline PEO (197 J/g[39]) yields the percent crystallinity of the specimen as presented in Table 1. As the crystallinity in the fibers is solely due to PEO, the proportion of weight of PEO in the fibers has been factored into when calculating the percent crystallinity. We find that addition of HASE to the 4% PEO solution decreases the crystallinity of the resulting fibers from 76.2% to 72.6%. The decrease in crystallinity becomes significant once NP15 surfactant is added to the precursor solution. A similar decrease in crystallinity is observed for the 3 wt % PEO system in the presence of HASE. The melt temperature is also found to follow the same trend as that of the % crystallinity. These results indicate that the presence of HASE and surfactant molecules interferes with the crystallization of PEO molecules thereby reducing the final crystallinity of the final fibers. Moreover, the decrease in crystallinity upon HASE addition is more pronounced for fibers spun from 3% PEO solutions. An interesting result to note from Table 1 is that the crystallinity of fibers electrospun from PEO-only solutions is slightly higher than that of the as received PEO powder. Although the reason behind this phenomena is still unclear, similar observations of a higher crystallinity in electrospun fibers have been made earlier by Kim et al.[40] in their study on electrospinning of gold nanoparticles with PEO.

Table 1. Percent Crystallinity and Melt Peak Temperature As Measured by DSC of Various Electrospun Polymer Systems

system	melt peak temperature (°C)	% crystallinity
PEO as received	65	74.8
4% PEO	66.5	76.2
3% PEO	67.9	80.28
4% PEO/0.2%HASE	63.2	72.6
4% PEO/0.2%HASE/20 mM surfactant	60.7	65.6
3% PEO/0.1% HASE	63.4	74.3

4. Summary

In this study, we have successfully incorporated associative polymers into nanofibers via electrospinning. Steady state and dynamic rheological experiments correlated the viscoelastic behavior of the precursor solutions with the properties of the resulting nanofibers. In particular, SEM micrographs indicate that the solution rheology puts a limit to the HASE concentration that can be electrospun. This problem can however be circumvented through use of nonionic surfactants as formation of poor quality beaded fibers could be transformed to production of defect-free nanofibers upon addition of surfactants to the precursor solution. Such significant improvement in the morphology of the nanofibers was primarily attributed to the change in solution viscoelasticity and in particular relaxation time, and not the solution viscosity. FTIR spectroscopy verified the presence of associative polymer and surfactants in the electrospun fibers. The presence of surfactants in particular appeared to significantly affect the crystallinity of the resulting nanofibers.

Acknowledgment. The authors gratefully acknowledge the Nonwovens Cooperative Research Center (NCRC) for funding this work.

References and Notes

(1) Reneker, D. H.; Chun, I. *Nanotechnology* **1996**, *7*, 216–223.
(2) Gibson, P.; Schreuder-Gibson, H.; Rivin, D. *Colloids Surf., A* **2001**, *187*, 469–481.
(3) Huang, Z. M.; Zhang, Y. Z.; Kotaki, M.; Ramakrishna, S. *Compos. Sci. Technol.* **2003**, *63*, 2223–2253.
(4) Khil, M. S.; Cha, D. I.; Kim, H. Y.; Kim, I. S.; Bhattarai, N. *J. Biomed. Mater. Res. B* **2003**, *67B*, 675–679.
(5) Li, D.; Xia, Y. *Adv. Mater.* **2004**, *16*, 1151–1170.
(6) Frenot, A.; Chronakis, I. S. *Curr. Opin. Colloid Interfaces* **2003**, *8* (1), 64–75.
(7) Dzenis, Y. *Science* **2004**, *304* (5679), 1917–1919.
(8) McKee, M. G.; Layman, J. M.; Cashion, M. P.; Long, T. E. *Science* **2006**, *311* (5759), 353–355.
(9) Sawicka, K. M.; Gouma, P. *J. Nanopart. Res.* **2006**, *8*, 769–781.
(10) Burger, C.; Hsiao, B. S.; Chu, B. *Annu. Rev. Mater. Res.* **2006**, *36*, 333–368.
(11) Teo, W. E.; Ramakrishna, S. *Nanotechnology* **2006**, *17* (14), R89–R106.

(12) Srinivasan, G.; Reneker, D. H. *Polym. Int*. **1995**, *36* (2), 195–201.
(13) Kim, J. S.; Reneker, D. H. *Polym Composite* **1999**, *20* (1), 124–131.
(14) Bergshoef, M. M.; Vancso, G. J. *Adv. Mater*. **1999**, *11*, 1362–1365.
(15) McKee, M. G.; Wilkes, G. L.; Colby, R. H.; Long, T. E. *Macromolecules* **2004**, *37*, 1760–1767.
(16) Shenoy, S. L.; Bates, W. D.; Wnek, G. *Polymer* **2005**, *46*, 8990–9004.
(17) Shenoy, S. L.; Bates, W. D.; Frisch, H. L.; Wnek, G. E. *Polymer* **2005**, *46*, 3372–3384.
(18) Yu, J. H.; Fridrikh, S. V.; Rutledge, G. C. *Polymer* **2006**, *47*, 4789–4797.
(19) Tirtaatmadja, V.; Tam, K. C.; Jenkins, R. D. *Macromolecules* **1997**, *30*, 3271–3282.
(20) English, R. J.; Gulati, H. S.; Jenkins, R. D.; Khan, S. A. *J. Rheol*. **1997**, *41*, 427–444.
(21) Kumacheva, E.; Rharbi, Y.; Winnik, M. A.; Guo, L.; Tam, K. C.; Jenkins, R. D. *Langmuir* **1997**, *13*, 182–186.
(22) Jenkins, R. D.; M., D. L.; Bassett, D. R. Influence of Alkali-Soluble Associative Emulsion Polymer Architecture on Rheology. In *Hydrophilic Polymers: Performance with Environmental Acceptance*; Glass, J. E.; Ed.; American Chemical Society: Washington, D. C., 1996; pp 425−447.
(23) English, R. J.; Laurer, J. H.; Spontak, R. J.; Khan, S. A. *Ind. Eng. Chem. Res*. **2002**, *41*, 6425–6435.
(24) Tam, K. C.; Seng, W. P.; Jenkins, R. D.; Bassett, D. R. *J. Polym. Sci., Polym. Phys*. **2000**, *38*, 2019–2032.
(25) Talwar, S.; Scanu, L. F.; Khan, S. A. *J. Rheol*. **2006**, *50*, 831–847.
(26) Tirtaatmadja, V.; Tam, K. C.; Jenkins, R. D. *AIChE J*. **1998**, *44*, 2756–2765.
(27) Tirtaatmadja, V.; Tam, K. C.; Jenkins, R. D. *Langmuir* **1999**, *15*, 7537–7545.
(28) Wu, W.; Olesen, K. R.; Shay, G. D.; Dockery, J. R. *Polym. Mater.: Sci. Eng*. **2001**, 85.
(29) Talwar, S.; Scanu, L. F.; Raghavan, S. R.; Khan, S. A. *Langmuir* **2008**, *24*, 7797–7802.
(30) Talwar, S.; Hinestroza, J.; Pourdeyhimi, B.; Khan, S. *Macromolecules* **2008**, *41*, 4275–4283.
(31) Tirtaatmadja, V.; Tam, K. C.; Jenkins, R. D.; Bassett, D. R. *Colloid Polym. Sci*. **1999**, *277* (2−3), 276–281.
(32) Abdala, A. A.; Tonelli, A. E.; Khan, S. A. *Macromolecules* **2003**, *36*, 7833–7841.
(33) Abdala, A. A.; Wu, W. J.; Olesen, K. R.; Jenkins, R. D.; Khan, S. A. *J. Rheol*. **2004**, *48*, 979–994.
(34) Jin, H. J.; Fridrikh, S. V.; Rutledge, G. C.; Kaplan, D. L. *Biomacromolecules* **2002**, *3*, 1233–1239.
(35) Carroll, C. P.; Joo, Y. L. *Phys. Fluids* **2006**, *18* (5).
(36) Thompson, C. J.; Chase, G. G.; Yarin, A. L.; Reneker *Polymer* **2006**, *48*, 6913–6922.
(37) Osman, Z.; Ansor, N. M.; Chew, K. W.; Kamarulzaman, N. *Ionics* **2005**, *11* (5−6), 431–435.
(38) Socrates, G. *Infrared and Raman Characteristic Group Frequencies: Tables and Charts*, 3rd ed.; Wiley: Chichester, NY, 2001.
(39) Wunderlich, B. *Thermal Analysis*; Academic Press: San Diego, CA, 1990; pp 417−431.
(40) Kim, G.-M.; Wutzler, A.; Radusch, H.-J.; Michler, G. H.; Simon, P.; Sperling, R. A.; Parak, W. J. *Chem. Mater*. **2005**, *17*, 4949–4957.